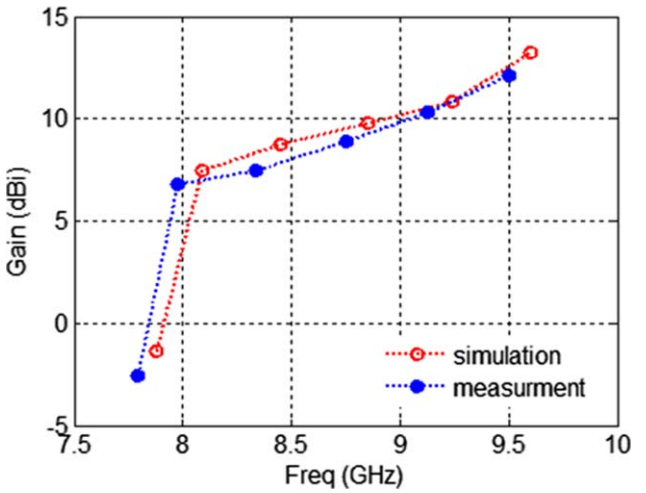

Figure 6 Variation of gain in first quarter (angular sector of $\theta = 0 \sim +90°$). [Color figure can be viewed in the online issue, which is available at wileyonlinelibrary.com]

advantages of compactness and simplicity of design, which make it suitable in radar and satellite communications.

ACKNOWLEDGMENT

The authors wish to express appreciation to Research Deputy of Ferdowsi University of Mashhad for supporting this project by grant No. 3/20770.

REFERENCES

1. P.N. Richardson and H.Y. Lee, Design and analysis of slotted waveguide arrays, Microwave J 31 (1988), 109–125.
2. S.R. Rengarajan, Compound radiating slots in a broad wall of a rectangular waveguide, IEEE Trans Antennas Propag 37 (1989), 1116–1123.
3. R.S. Rengarajan, Compound coupling slots for arbitrary excitation of waveguide-fed planar slot arrays, IEEE Trans Antennas Propag 38 (1990), 276–280.
4. J.C. Coetzee, Off-center-frequency analysis of a complete planar slotted-waveguide array consisting of subarrays, IEEE Trans Antennas Propag 48 (2000), 1746–1755.
5. L. Yan, W. Hong, G. Hua, J.X. Chen, K. Wu, and T.J. Cui, Simulation and experiment on SIW slot array antennas, IEEE Microwave Wirel Compon Lett 14 (2004), 446–448.
6. Z.B. Weng, R. Gou, and Y.C. Jiao, Design and experiment on Substrate integrated waveguide resonant slot array antenna at KU-band, In: International Symposium on Antennas Propagation and EM Theory, 2006, pp. 1–3.
7. Z. Chen, W. Hong, Z. Kuai, H. Tang, and J. Chen, 45° linearly polarized resonant slot array antenna based on substrate integrated waveguide, In: Asia-Pacific Microwave Conference Proceeding, Bangkok, Thailand, 2007, pp. 1–4.
8. P. Chen, W. Hong, Z. Kaui, and J. Xu, A substrate integrated waveguide circular polarized slot radiator and its linear array, IEEE Antennas Wirel Propag Lett 8 (2009), 120–123.
9. W. Hong, Development of microwave antennas, components and subsystems based on SIW technology, In: IEEE international symposium on Microwave Antenna Propagation and EMC Technologies, 2005, pp. 14–17.
10. F. Xu and K. Wu, Guided-wave and leakage characteristics of substrate integrated waveguide, IEEE Trans Microwave Theory Tech 53 (2005), 66–73.
11. G.Q. Luo, W. Hong, Q.H. Lai, K. Wu, and L.L. Sun, Design and experimental verification of compact frequency selective surface with quasi-elliptic bandpass response, IEEE Trans Microwave Theory Tech 55 (2007), 2481–2487.
12. H. Uchimura, T. Takenoshita, and M. Fujii, Development of a "Laminated Waveguide", IEEE Trans Microwave Theory Tech 46 (1998), 2438–2443.

PRINTED DUAL-FEED TRIANGULAR PATCH ANTENNA DISPOSED IN A SMALL NOTCH IN THE HANDHELD DEVICE SYSTEM GROUND PLANE FOR LTE/WWAN OPERATION

Yi-Ting Hsieh,[1] Kin-Lu Wong,[1] Yung-Tao Liu,[2] and Hong-Twu Chen[2]

[1] Department of Electrical Engineering, National Sun Yat-Sen University, Kaohsiung 804, Taiwan

[2] Department of Electrical Engineering, R.O.C. Military Academy, Kaohsiung 830, Taiwan; Corresponding author: wongkl@ema.ee.nsysu.edu.tw

Received 10 March 2013

ABSTRACT: *A printed triangular patch antenna disposed in a small notch at one corner of the system ground plane of the handheld communication device such as the smartphone, tablet computer, and phone tablet for long term evolution/wireless wide area network (LTE/WWAN) operation is presented. The small notch has a size of 10 × 20 mm^2 only, and two tips of the triangular patch disposed therein are in close proximity to two adjacent perpendicular edges of the notch. The two tips are the antenna's two feeds for achieving LTE/WWAN operation. Each tip can be connected to an ON/OFF switch (e.g., a PIN diode) such that the antenna can be controlled to be fed at either the first or the second tip. When fed at the first tip, the antenna will operate in a high-frequency band (1710–2690 MHz) to cover the GSM1800/1900/UMTS/LTE2300/2500 operation. When fed at the second tip and aided by a matching circuit, the antenna will operate at a low-frequency band (824–960 MHz) to cover the GSM850/900 operation. Design considerations of the proposed antenna are described. Parametric studies and experimental results of the antenna are presented and discussed.* © 2013 Wiley Periodicals, Inc. Microwave Opt Technol Lett 55:2767–2773, 2013; View this article online at wileyonlinelibrary.com. DOI 10.1002/mop.27910

Key words: *mobile antennas; long term evolution/wireless wide area network antennas; small antennas; smartphone antennas; tablet computer antennas*

1. INTRODUCTION

For modern handheld communication devices such as the smartphone, tablet computer, and phone tablet with a slim profile or very thin thickness, the internal long term evolution/wireless wide area network (LTE/WWAN) antennas embedded therein are accordingly required to be of small size and low profile as well. Further, to achieve wideband or multiband operation, the embedded antennas are required to be disposed in a clearance or no-ground region of the system circuit board [1–4]. In this case, an isolation distance between the antenna's metal pattern and the nearby ground plane is also required to minimize the coupling effects of the ground plane on the impedance matching of the embedded antenna. This requirement requires an additional board space for the embedded antenna and hence increases the total occupied volume of the embedded antenna inside the handheld device.

To decrease or minimize the antenna's total occupied volume which comprises the antenna's metal pattern and the required isolation space, it becomes attractive that the embedded

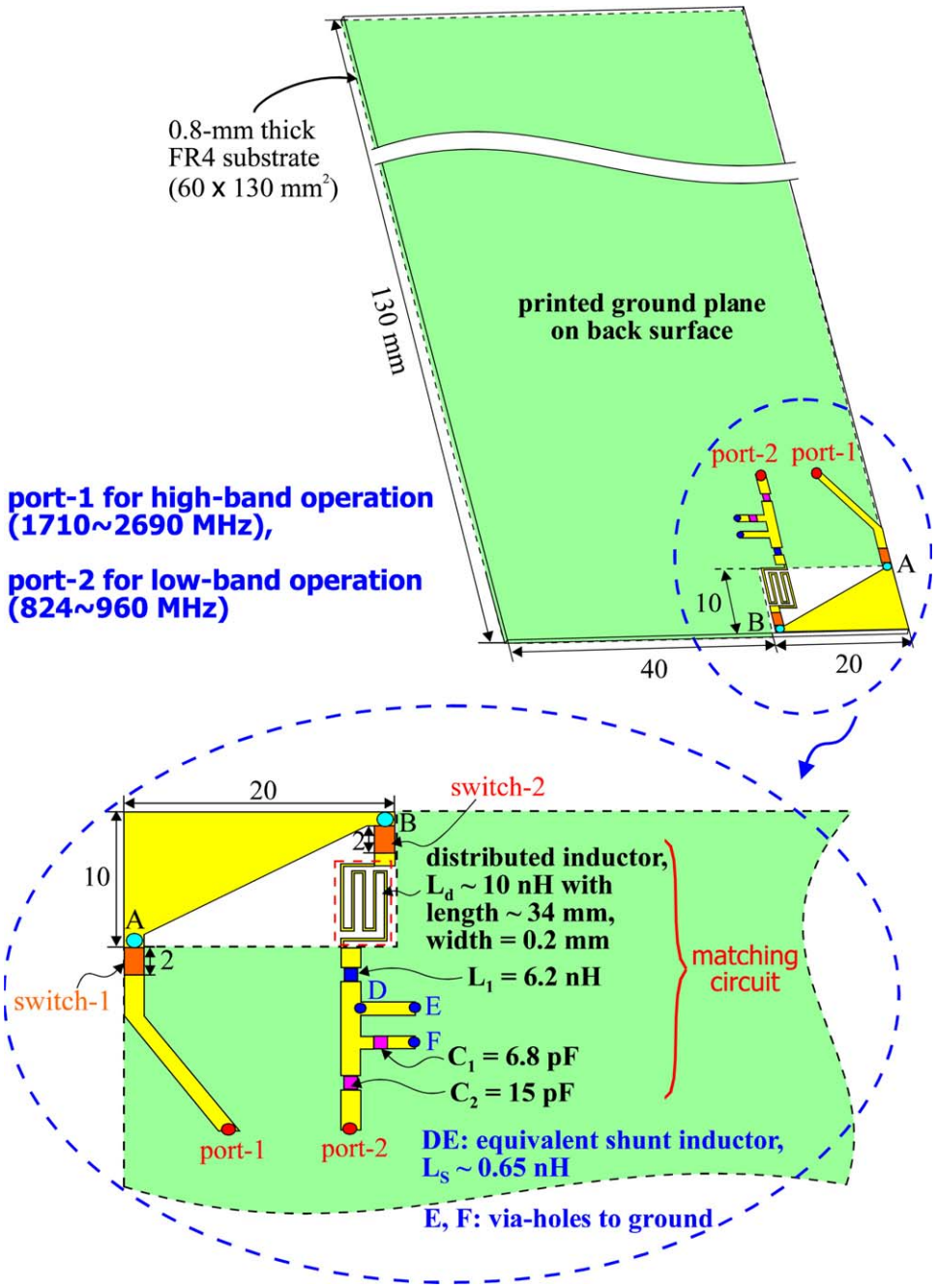

Figure 1 Geometry of the on-board printed dual-feed triangular patch antenna for the LTE/WWAN application in a smartphone. [Color figure can be viewed in the online issue, which is available at wileyonlinelibrary.com]

antennas can be closely integrated with the system ground plane of the handheld device. Some promising WWAN antennas that are capable of close integration with nearby ground plane in the mobile handset have been reported [5–11]. In Ref. 5, the penta-band WWAN antenna (824–960/1710–2170 MHz) is an on-board printed coupled-fed loop antenna disposed in a small no-ground region (15×25 mm^2) of the system ground plane. The antenna is closely integrated with the nearby ground plane, and there is generally no isolation space required between the antenna's metal pattern and the nearby ground plane such that the antenna's total required board space on the system circuit board is decreased. Similar design considerations applied to a small notch at a corner [6–8] or in the middle [9–11] of an edge of the handheld device system ground plane have also been reported. Such internal antennas have the advantages of close integration with associated electronic elements such as the USB connector which serves as a data interface with external devices [12–16]. This advantageous property can lead to compact integration of the embedded antennas inside the handheld devices.

In this article, we report an on-board printed dual-feed triangular patch antenna that can be disposed in a small notch (10×20 mm^2) at one corner of the system ground plane of the handheld device such as the smartphone, tablet computer, and phone tablet for the LTE/WWAN operation. The antenna size or the notch size is only about 53% of the reported antennas in Refs. 5 and 6 in which the antennas have a planar structure and are

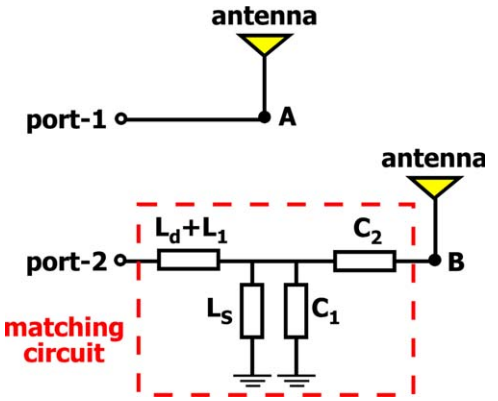

Figure 2 Equivalent circuits for port-1 excitation (switch-1 ON, switch-2 OFF) and port-2 excitation (switch-1 OFF, switch-2 ON). [Color figure can be viewed in the online issue, which is available at wileyonlinelibrary.com]

printed on-board inside a notch of size 15 × 25 mm^2. The much smaller antenna size makes the proposed antenna more attractive for modern slim handheld device applications.

In the proposed antenna, the two tips of the triangular patch are in close proximity to two adjacent perpendicular edges of the small notch. The two tips are the antenna's two feeds for achieving LTE/WWAN operation. Each tip can be connected to an ON/OFF switch (e.g., a PIN diode for the switch [17–19]) such that the antenna can be controlled to be fed at either the first or the second tip. To simplify the manufacturing process and focus on the operating principle of the proposed antenna, the switching diode is simulated as a metal strip for its ON state (forward-biased state) and as an open gap for its OFF state (reverse-biased state) [19,20]. The obtained results for the antenna with the PIN diodes have also been reported to show small variations as compared to the same antenna using a conducting strip to mimic the PIN diode [19].

When the antenna is fed at the first tip, it will operate in a high-frequency band of 1710–2690 MHz to cover the GSM1800/1900/UMTS/LTE2300/2500 operation. Conversely, when the antenna is fed at the second tip, it will operate in a low-frequency band of 824–960 MHz to cover the GSM850/900 operation, although the triangular patch can provide a maximum resonant path of 30 mm only (about 0.09 wavelength at 900 MHz). The excitation of the wideband resonant mode in the desired low-frequency band is mainly owing to the use of a matching circuit [21] which includes the use of a series inductance to shift the resonant mode to be at about 900 MHz, a bandpass matching circuit of shunt inductance and capacitance to achieve dual-resonance excitation for bandwidth enhancement, and a series capacitance to fine adjust the impedance matching of the excited dual-resonance mode. Hence, with a very small total occupied size of 10 × 20 mm^2 which includes the antenna and its required clearance, the antenna with a planar structure in this study can provide two operating bands of 824–960 and 1710–2690 MHz for the LTE/WWAN operation. Details of the proposed antenna are described, and design considerations and experimental results of the proposed antenna are presented.

2. PROPOSED ANTENNA

Figure 1 shows the geometry of the proposed printed dual-feed triangular patch antenna for the LTE/WWAN application in a smartphone. The triangular patch is printed inside a small notch of 10 × 20 mm^2 at a corner of the system ground plane of the

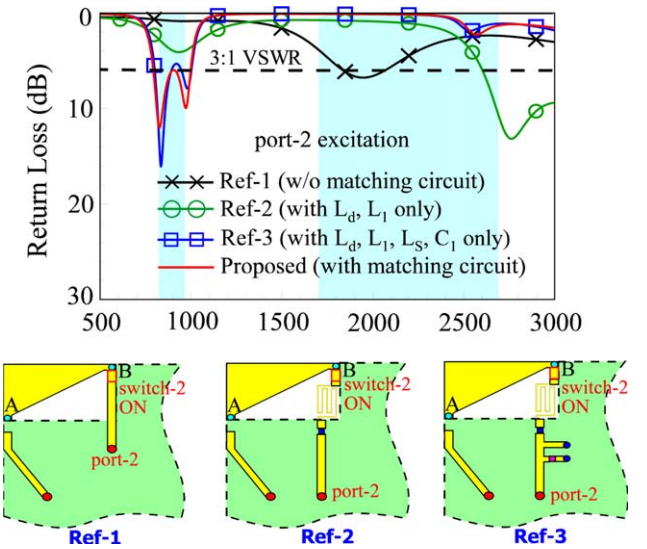

Figure 3 Simulated return loss with and without the matching circuit for port-2 excitation. [Color figure can be viewed in the online issue, which is available at wileyonlinelibrary.com]

smartphone. The two side edges of the triangular patch are 10 and 20 mm in length and are flushed to the two adjacent edges of the corner. The system ground plane in this study is simulated as the printed ground plane on the back surface of a 0.8-mm thick FR4 substrate of size 130 × 60 mm^2, which are reasonable dimensions for modern smartphones.

The two tips (point A and B) of the triangular patch are the antenna's two feeds for achieving LTE/WWAN operation. Point A is connected to switch-1 for port-1 excitation to cover the high-band operation of 1710–2690 MHz, whereas point B is connected to switch-2 and a matching circuit for port-2 excitation to

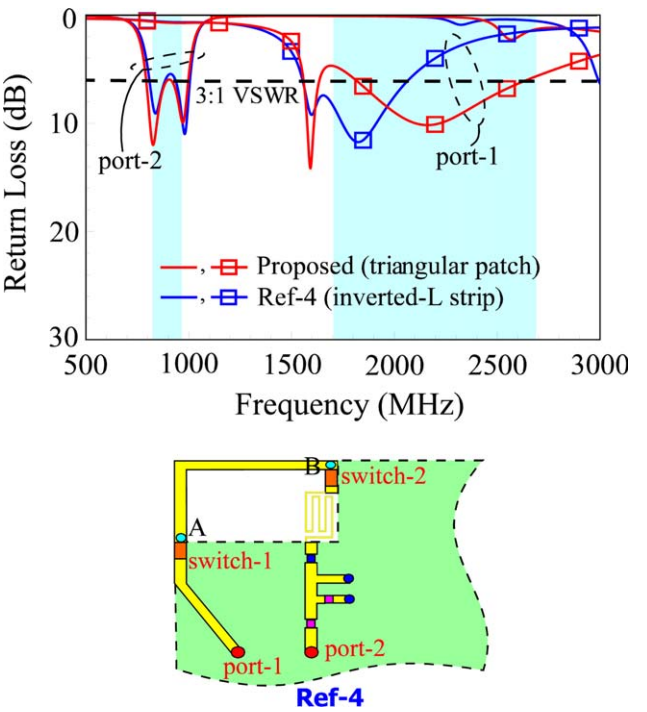

Figure 4 Simulated return loss for the proposed antenna and the case with an inverted-L strip. [Color figure can be viewed in the online issue, which is available at wileyonlinelibrary.com]

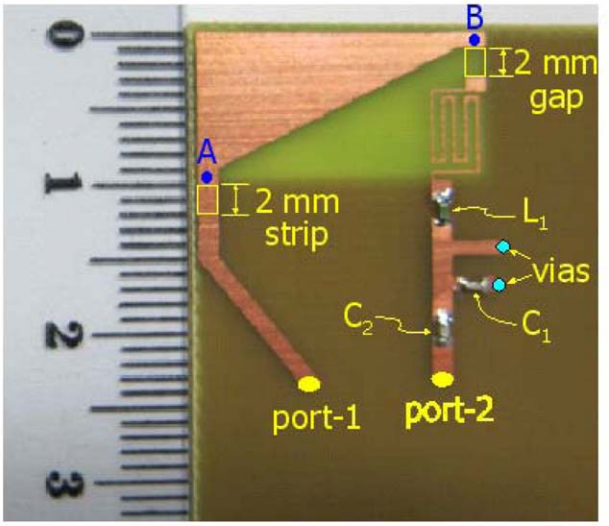

(a) port-1 excitation

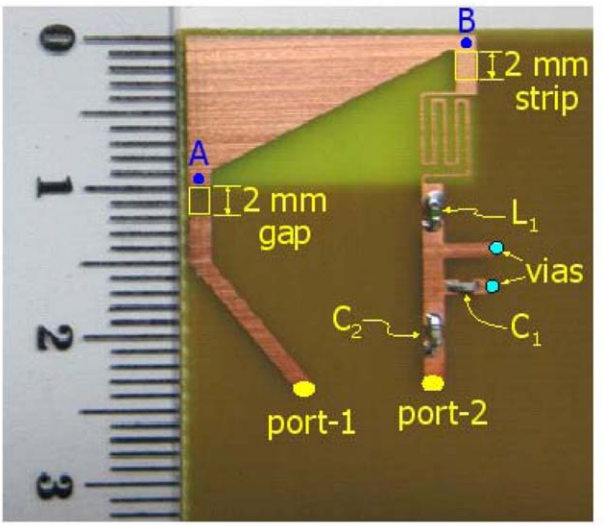

(b) port-2 excitation

Figure 5 Photos of the fabricated antenna; the switches to be connected to the two tips of the printed triangular patch are replaced by a 2-mm long metal strip for the ON state and a 2-mm long gap for the OFF state. (a) Port-1 excitation and (b) port-2 excitation. [Color figure can be viewed in the online issue, which is available at wileyonlinelibrary.com]

cover the low-band operation of 824–960 MHz. The equivalent circuits for port-1 and port-2 excitation of the proposed antenna are shown in Figure 2. The matching circuit includes a series inductor of L_d and L_1, a band-pass matching circuit of shunt inductor L_S and shunt capacitor C_1, and a series capacitor C_2. The series inductors of L_d and L_1 are used to shift the antenna's fundamental resonant mode to occur at about 900 MHz. Note that a single low-loss chip inductor of about 16.2 nH is also suitable to replace L_d and L_1 in this study. The distributed inductor L_d is formed by a long, narrow strip of length about 34 mm printed inside the notch, which has an equivalent inductance of about 10 nH. With the presence of L_d, a chip inductor of lower inductance 6.2 nH (L_1) can be used. In this case, simple chip inductors can be applied as the possible ohmic losses associated with the chip inductor with a smaller inductance is generally small, and its effects on the antenna efficiency can be neglected.

For the shunt inductor L_S (~0.65 nH) and shunt capacitor C_1 (6.8 pF), they can lead to a dual-resonance excitation of the resonant mode at about 900 MHz, hence resulting in bandwidth enhancement of the antenna's low-band operation. Note that, as the required shunt inductance is small (less than 1 nH), a simple shorting strip can be applied as shown in Figure 1 to provide an equivalent inductance of about 0.65 nH required in the proposed design, and an additional chip inductor is not necessary. The series capacitor C_2 (15 pF) is used for fine-adjusting the impedance matching of the dual-resonance excitation of the resonant mode at about 900 MHz such that the desired low band can cover the GSM850/900 operation (824–960 MHz). Detailed effects of the matching circuits will be analyzed with the aid of Figure 3 in Section 3.

For port-1 excitation, no matching circuit is required, and the excited fundamental resonant mode of the triangular patch can provide a wide bandwidth to cover the GSM1800/1900/UMTS/LTE2300/2500 operation (1710–2690 MHz). It should be noted that when using a patch with a smaller width (e.g., an inverted-L strip as studied in Fig. 4 in Section 3) to replace the triangular patch in the proposed design, the bandwidth of the antenna's high-band operation will be greatly decreased and cannot cover the desired operating band of 1710–2690 MHz. The related results will be discussed in Section 3 with the aid of Figure 4.

It is also noted that as reported in Ref. 19, the switches are suitable to be simulated as a conducting strip for its ON state and as an open gap for its OFF state to simplify the study. Hence, for port-1 excitation, switch-1 in the ON state is simulated as a 2-mm long metal strip, with switch-2 in the OFF state simulated as a 2-mm long gap [see the photo of the fabricated antenna in Fig. 5(a)]. For port-2 excitation, switch-1 in the OFF state is simulated as a 2-mm long gap, with switch-2 in the ON state simulated as a 2-mm long metal strip [see the photo of the fabricated antenna in Fig. 5(b)]. The experimental results and parametric studies of the proposed design are presented in the next section.

3. RESULTS AND DISCUSSION

The fabricated antennas shown in Figure 5 were tested. Figure 6 shows the measured and simulated return loss for port-1 and port-2 excitation. The simulated results are obtained using the full-wave electromagnetic field simulator HFSS version 14 [22]. Good agreement between the measured data and simulated results is observed. The low-band operation controlled by port-2 excitation covers the GSM850/900 operation (the shaded frequency range at about 900 MHz in the figure), whereas the

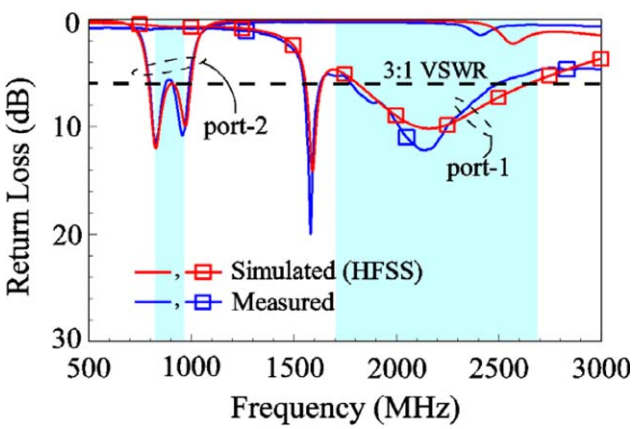

Figure 6 Measured and simulated return loss for port-1 and port-2 excitation. [Color figure can be viewed in the online issue, which is available at wileyonlinelibrary.com]

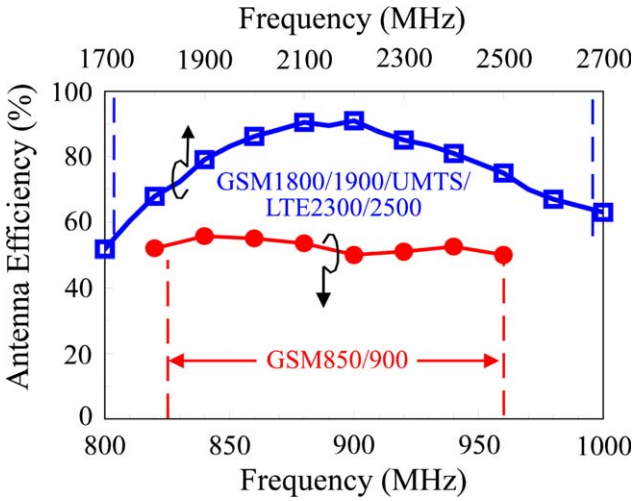

Figure 7 Measured antenna efficiency (return losses included) of the fabricated antenna. [Color figure can be viewed in the online issue, which is available at wileyonlinelibrary.com]

high-band operation controlled by port-1 excitation covers the GSM1800/1900/UMTS/LTE2300/2500 operation (the shaded frequency range at higher frequencies in the figure). Over the operating bands, the impedance matching is better than 6 dB (3:1 VSWR), which is widely used as the design specification for internal LTE/WWAN antennas.

The measured antenna efficiency which includes the return losses is shown in Figure 7. It is seen that the antenna efficiency in the low band and high band is about 50–55% and 55–90%, respectively, which is acceptable for practical smartphone applications. It is also noted that for port-2 excitation, a resonant mode at about 1.6 GHz outside the desired high band is excited, which is mainly owing to the printed long narrow strip for the distributed inductor to be parasitically excited. This resonant mode at about 1.6 GHz does not affect the high-band operation of the antenna.

Figure 8 shows the measured radiation patterns of the fabricated antenna. The full three-dimensional radiation patterns and cross-sectional views seen in the *y-z* plane are shown. At 900 MHz, a dipole-like radiation pattern is seen. This indicates that the surface currents excited on the system ground plane still dominate the radiation at lower frequencies, which is similar to the observations at lower frequencies at about 900 MHz for

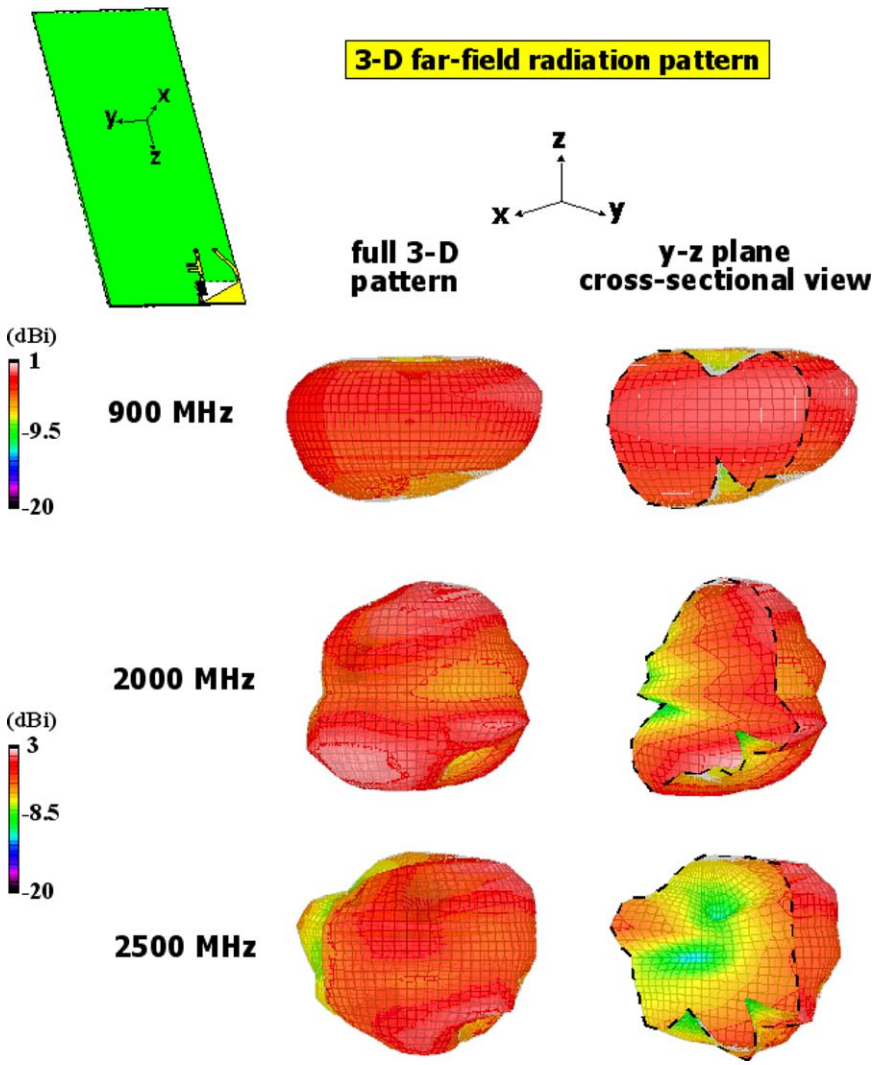

Figure 8 Measured radiation patterns of the fabricated antenna. [Color figure can be viewed in the online issue, which is available at wileyonlinelibrary.com]

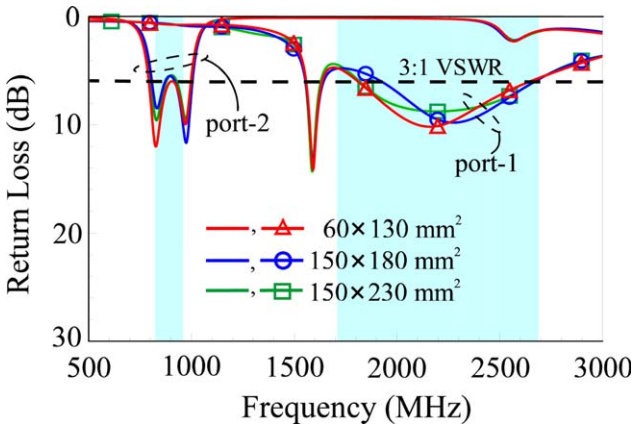

Figure 9 Simulated return loss for the proposed antenna with different ground plane sizes. [Color figure can be viewed in the online issue, which is available at wileyonlinelibrary.com]

traditional handset antennas [23]. At 2000 and 2500 MHz, the representative frequencies in the high band, the radiation patterns show relatively stronger radiation in the $+y$ direction, although the antenna is disposed at the corner facing the $-y$ direction. This also suggests that the surface currents excited on the system ground plane still contribute greatly to the measured radiation patterns, even at frequencies in the high band. It is noted that for practical applications, owing to the small size of the proposed LTE/WWAN antenna, a second antenna can be disposed in a second small notch at the lower left corner facing the $+y$ direction to form an antenna array to perform diversity operation or LTE multi-input multioutput operation [13].

Effects of the matching circuit are also analyzed. Figure 3 shows the simulated return loss with and without the matching circuit for port-2 excitation. Ref-1 is for the case without the matching circuit. Ref-2 is for the case with the series inductor of L_d and L_1 only, whereas Ref-3 is for the case with L_d, L_1, and the shunt elements L_S and C_1 only. For Ref-1, it is seen that the excited resonant mode occurs at about 2 GHz in the high band, far from the desired frequencies at about 900 MHz. This is because the maximum resonant length provided by the triangular patch is 30 mm only, far less than the required 0.25 wavelength of the frequencies in the desired low band. With the presence of L_d and L_1 (Ref-2), a resonant mode can be generated at about 900 MHz. With the aid of further adding L_S and C_1 (Ref-3), dual-resonance excitation for this resonant mode can be obtained, and the obtained bandwidth is wide enough for the desired low band. The dual-resonance excitation is similar to those obtained using a parallel-resonance spiral slit or strip [24,25] or a bandstop matching circuit [26,27] for bandwidth enhancement. Finally, the adding of C_2 (proposed design) can improve the impedance matching of the obtained low band for Ref-2.

Effects of the ground plane dimensions on the proposed antenna are also studied. Figure 9 shows the simulated return loss for the proposed antenna with different ground plane sizes. Results for two different ground planes (size 150 × 180 mm^2 and 150 × 230 mm^2 for tablet computers or phone tablets) other than the one shown in Figure 1 are presented. Small variations in the return loss for both port-1 and port-2 excitation are seen. This suggests that the proposed antenna is not sensitive to the ground size variations, which makes it easy to be applied to smartphones or tablet computers or phone tablets.

Figure 4 shows the simulated return loss for the proposed antenna with a triangular patch and the case with an inverted-L strip (Ref-4). Small variations in the return loss for low-band operation are observed. This suggests that the wideband operation of the low band is mainly owing to the matching circuit added for port-2 excitation. For the high band, however, large variations in the impedance matching are seen, and the obtained bandwidth for Ref-4 is much smaller compared to the proposed antenna. This indicates that the use of a triangular patch which has a much wider strip width than the inverted-L strip can lead to the excitation of a wideband resonant mode to cover the desired high-band operation.

4. CONCLUSION

A dual-feed triangular patch antenna disposed in a small notch at one corner of the handheld device system ground plane for the LTE/WWAN operation has been proposed. The proposed antenna has a simple structure and a small size as well, yet it can provide two wide operating bands to cover the 824–960 and 1710–2690 MHz bands for the LTE/WWAN operation. The notch has a small size of 10 × 20 mm^2 only, which is enough to accommodate the triangular patch and provide the required clearance for the antenna to the adjacent system ground plane. The operating principle of the proposed antenna has been discussed, and the measured results of the fabricated antenna have also been presented. The obtained antenna performances including the impedance matching and antenna efficiency in the desired low-band and high-band operations are acceptable for practical applications in the smartphones or tablet computers or phone tablets.

REFERENCES

1. Y.W. Chi and K.L. Wong, Compact multiband folded loop chip antenna for small-size mobile phone, IEEE Trans Antennas Propag 56 (2008), 3797–3803.
2. J.H. Kim, W.W. Cho, and W.S. park, A small printed dual-band antenna for mobile phones, Microwave Opt Technol Lett 51 (2009), 1699–1702.
3. K.L. Wong and S.C. Chen, Printed single-strip monopole using a chip inductor for penta-band WWAN operation in the mobile phone, IEEE Trans Antennas Propag 58 (2010), 1011–1014.
4. M.H. Seko and F.S. Correra, A novel tri-band planar inverted-F antenna for GSM/DCS/PCS operation in mobile handsets, Microwave Opt Technol Lett 55 (2013), 821–825.
5. K.L. Wong, W.Y. Chen, and T.W. Kang, On-board printed coupled-fed loop antenna in close proximity to the surrounding ground plane for penta-band WWAN mobile phone, IEEE Trans Antennas Propag 59 (2011), 751–757.
6. S. Yang, Y.L. Band, and J. Li, On-board printed coupled-fed antenna for hexa-band WWAN/LTE mobile phone, In: International Workshop on Electromagnetics (iWEM): Applications and Student Innovation, Taipei, Taiwan, 2012, pp. 1–2.
7. S.C. Chen and K.L. Wong, Small-size wideband chip antenna for WWAN/LTE operation and close integration with nearby conducting elements in the mobile handset, Microwave Opt Technol Lett 53 (2011), 1998–2004.
8. K.L. Wong, M.F. Tu, C.Y. Wu, and W.Y. Li, On-board 7-band WWAN/LTE antenna with small size and compact integration with nearby ground plane in the mobile phone, Microwave Opt Technol Lett 52 (2010), 2847–2853.
9. S.C. Chen and K.L. Wong, Low-profile, small-size, wireless wide area network handset antenna close integration with surrounding ground plane, Microwave Opt Technol Lett 54 (2012), 623–629.
10. F.H. Chu and K.L. Wong, Internal coupled-fed loop antenna integrated with notched ground plane for WWAN operation in the mobile handset, Microwave Opt Technol Lett 54 (2012), 599–605.
11. K.L. Wong, Y.C. Kao, and F.H. Chu, Small-size WWAN handset antenna disposed at a small notch in the system ground plane, Microwave Opt Technol Lett 54 (2012), 2498–2503.

12. F.H. Chu and K.L. Wong, Internal coupled-fed dual-loop antenna integrated with a USB connector for WWAN/LTE mobile handset, IEEE Trans Antennas Propag 59 (2011), 4215–4221.
13. K.L. Wong, T.W. Kang, and M.F. Tu, Antenna array for LTE/WWAN and LTE MIMO operations in the mobile phone, Microwave Opt Technol Lett 53 (2011), 1569–1573.
14. K.L. Wong and Y.W. Chang, Internal WWAN/LTE handset antenna integrated with USB connector, Microwave Opt Technol Lett 54 (2012), 1154–1159.
15. F.H. Chu and K.L. Wong, On-board small-size printed LTE/WWAN mobile handset antenna closely integrated with nearby system ground plane, Microwave Opt Technol Lett 53 (2011), 1336–1343.
16. K.L. Wong and C.H. Chang, On-board small-size printed monopole antenna integrated with USB connector for penta-band WWAN mobile phone, Microwave Opt Technol Lett 52 (2010), 2523–2527.
17. E. Palantei, D.V. Thiel, and S.G. O'Keefe, Rectangular patch with parasitic folded dipoles: A reconfigurable antenna, In: International Workshop on Antenna Technology (iWAT), Chiba, Japan, 2008, pp. 251–254.
18. S.H. Chen, J.S. Row, and K.L. Wong, Reconfigurable square-ring patch antenna with pattern diversity, IEEE Trans Antennas Propag 55 (2009), 472–475.
19. Y.K. Park and Y. Sung, A reconfigurable antenna for quad-band mobile handset applications, IEEE Trans Antennas Propag 60 (2012), 3003–3006.
20. Q. Luo, J.R. Pereira, and H.M. Salgado, Reconfigurable dual-band C-shaped monopole antenna array with high isolation, Electron Lett 46 (2010), 888–889.
21. Andújar and J. Anguera, Multiband coplanar ground plane booster antenna technology, Electron Lett 48 (2012), 1326–1328.
22. ANSYS HFSS, Available at: http://www.ansys.com/products/hf/hfss/.
23. K.L. Wong, Planar antennas for wireless communications, Wiley, New York, 2003.
24. K.L. Wong, Y.W. Chang, and S.C. Chen, Bandwidth enhancement of small-size WWAN tablet computer antenna using a parallel-resonant spiral slit, IEEE Trans Antennas Propag 60 (2012), 1705–1711.
25. K.L. Wong, T.J. Wu, and P.W. Lin, Small-size uniplanar WWAN tablet computer antenna using a parallel-resonant strip for bandwidth enhancement, IEEE Trans Antennas Propag 61 (2013), 492–496.
26. Y.W. Chi and K.L. Wong, Very-small-size folded loop antenna with a band-stop matching circuit for WWAN operation in the mobile phone, Microwave Opt Technol Lett 51 (2009), 808–814.
27. K.L. Wong and P.J. Ma, Small-size WWAN monopole slot antenna with dual-band band-stop matching circuit for tablet computer application, Microwave Opt Technol Lett 54 (2012), 875–879.

A BiCMOS Ka-BAND RF-PULSE FORMER FOR SHORT-RANGE HIGH-RESOLUTION RADAR AND HIGH-DATA-RATE COMMUNICATION SYSTEMS

Cuong Huynh and Cam Nguyen
Department of Electrical and Computer Engineering, Texas A&M University, College Station, TX 77843-3128; Corresponding author: cuonghpm@tamu.edu

Received 14 March 2013

ABSTRACT: *An ultra-low-leakage RF-pulse former capable of producing very narrow RF pulses with small rising and falling time for short-range high-resolution radar and high-data-rate communication systems is developed using 0.18-μm BiCMOS technology. The narrow RF pulses are produced from a continuous-wave RF signal by gating a high-speed single-pole single-throw switch implemented with small gate-resistors. The RF-pulse former exhibits an extremely low RF leakage implementing the RF leaking suppression technique, in which the RF leaking signal is cancelled by combining with its replica using an active balun. In addition, the active balun also amplifies the gated RF pulses hence providing gain for the RF-pulse former. A graphical analysis based on the insertion loss and isolation contours, enabling selection of the optimum sizes for transistors in the series-shunt switches, is also presented. From 31 to 37.1 GHz, the designed RF-pulse former exhibits −1.9 dB (loss) to 1.1 dB (gain) and 14.5–30-dB input return loss. The output return loss is higher than 10 dB from 33 to 35.9 GHz. From 30 to 40 GHz, the isolation is higher than 40 dB and, especially at 34 GHz, the isolation reaches 70 dB. The rising and falling times were measured as 136 and 70 ps, respectively. Very narrow RF pulses of 200 ps have been generated. The RF-pulse former consumes a 7.3 mA from a 1.8-V power supply and occupies a chip area of 0.225 mm^2.* © 2013 Wiley Periodicals, Inc. Microwave Opt Technol Lett 55:2773–2777, 2013; View this article online at wileyonlinelibrary.com. DOI 10.1002/mop.27931

Key words: *RF-pulse former; pulsed radar; switch; BiCMOS; radio frequency integrated circuit*

1. INTRODUCTION

RF-pulse formers, based on time-gated STSP switches, are one of the most critical components in short-range, high-resolution pulse radar, and high-data-rate communication systems. RF-pulse formers with small switching time and high isolation are desirable for high range-resolution, accuracy, and receiver's dynamic range (hence detection range) in radar systems. Short-range high-resolution RF-pulse-based radar systems, such as those for automotive, are required to detect objects from few centimeters to several tens of meters in range with range accuracy and resolution smaller than 10 cm [1]. This leads to the need of RF-pulse formers capable of producing very narrow RF pulses with small rising and falling time. For communication systems, narrow RF pulses are needed to transmit and receive data at high rates. In addition, the RF-pulse formers in the transmitters are also required to have a very high isolation so that the transmitting signals can comply with the regulated spectrums and the system's dynamic range can be enhanced. It is desirable to have low insertion loss or possible gain for the RF-pulse formers as well.

Various fully integrated short-range radar systems, based on different techniques including impulse, RF pulse, and time correlation receiver using different technologies of III-V semiconductor, SiGe, CMOS, and BiCMOS, have been reported [1–4]. These systems use different transmit and receive antennae, with the transmitter (TX) and receiver (RX) located either on the same chip or different chips to maximize the system dynamic range. In order to reduce the system's cost and size, one antenna for both transmission and reception should be used along with a high-isolation T/R switch (or circulator) and RF-pulse former.

RF-pulse formers having ultrahigh isolation are highly desired for systems. To illustrate the need of high-isolation RF-pulse formers, we consider in Figure 1 a time-gated correlation transceiver architecture using one antenna for short-range radar systems, which is modified from the architecture presented in Ref. 1. The power amplifier (PA) may be on all the time for short-range and high-resolution applications. The operation of the transceiver is controlled by the TX-pulse and RX-pulse signals. In the transmission mode, a very narrow RF pulse, setting the range resolution for the system, is produced from the TX RF-pulse former by gating the signal from the continuous wave (CW) source, amplified by the PA, passes through the T/R switch, and transmitted by the antenna. In the reception mode, the reflected RF pulse from the target, after captured by the antenna and amplified by the low